

Anisotropic Electron Tail Generation during Tearing Mode Magnetic Reconnection

Ami M. DuBois,^{*} Abdulgader F. Almagri, Jay K. Anderson, Daniel J. Den Hartog, John David Lee, and John S. Sarff
Department of Physics, University of Wisconsin–Madison, Madison, Wisconsin 53706, USA

(Received 19 August 2016; published 14 February 2017)

The first experimental evidence of anisotropic electron energization during magnetic reconnection that favors a direction perpendicular to the guide magnetic field in a toroidal, magnetically confined plasma is reported in this Letter. Magnetic reconnection plays an important role in particle heating, energization, and transport in space and laboratory plasmas. In toroidal devices like the Madison Symmetric Torus, discrete magnetic reconnection events release large amounts of energy from the equilibrium magnetic field. Fast x-ray measurements imply a non-Maxwellian, anisotropic energetic electron tail is formed at the time of reconnection. The tail is well described by a power-law energy dependence. The expected bremsstrahlung from an electron distribution with an anisotropic energetic tail ($v_{\perp} > v_{\parallel}$) spatially localized in the core region is consistent with x-ray emission measurements. A turbulent process related to tearing fluctuations is the most likely cause for the energetic electron tail formation.

DOI: 10.1103/PhysRevLett.118.075001

Magnetic reconnection (MR) is characterized by impulsive, discrete bursts of released magnetic energy (U_{mag}). The release of U_{mag} and conversion to kinetic energy, plays an important role in particle transport and energization (heating and acceleration) in space and laboratory plasmas. In particular, electron energization during MR has been observed in the magnetotail [1–3], during magnetospheric substorms [4,5], during solar flares [6,7], and in laboratory experiments [8–15]. However, the mechanisms leading to the onset of MR and the energization of particles are not fully understood.

One of the major outstanding questions for electron acceleration during MR is whether the process is localized inside or outside of the diffusion region. The WIND spacecraft provided the first evidence of electron acceleration localized to the diffusion region, where the power-law spectra were more energetic compared to the outflow region and favors directions parallel or antiparallel to the guide field [3]. The symmetry between the parallel and antiparallel spectra suggests electrons may be energized by a process other than parallel electric fields in the diffusion region. It was later confirmed by CLUSTER that electrons can be accelerated by pitch angle scattering [16]. Relative to space-based observations, where *in situ* measurements are challenging, laboratory experiments provide a controlled environment to study electron energization during MR. Electron energization is commonly observed during the internal kink mode sawtooth cycle in tokamak plasmas. Parallel and antiparallel anisotropy in x-ray emission from nonthermal electrons, attributed to runaway acceleration driven by the inductive electric field created during the impulsive sawtooth crash, has been measured in the T-10 [10], VTF [8], TCV [9], and PLT [11] tokamaks.

This Letter presents the first experimental evidence for anisotropic electron energization during MR that favors a direction perpendicular to the mean (or guide) magnetic

field in a toroidal, magnetically confined plasma. The anisotropy appears as a nonthermal tail in the x-ray energy spectrum during MR events in reversed field pinch (RFP) plasmas. The x-ray tail fits a power law that flattens during MR. Runaway energization is ruled out by measured parallel or antiparallel symmetry in the x-ray flux. This is also the first evidence that electron energization accompanies the better-studied ion energization during MR in RFP plasmas [17,18].

The experiments described below were performed in the MST [19] RFP experiment having a major radius $R = 1.5$ m and a minor radius $a = 0.52$ m. MR in RFP plasmas stems from several tearing modes that are destabilized by the parallel current density gradient, and the nonlinear interaction between stable and unstable modes results in a quasiperiodic magnetic relaxation cycle that causes a sudden release of stored U_{mag} during the fast ($\sim 100 \mu\text{s}$) crash phase [20]. This cycle resembles the internal kink mode sawtooth process in tokamak plasmas in some respects, but it is more global in RFP plasmas due to its multimode nature. The overlap of magnetic islands from multiple tearing modes leads to widespread magnetic stochasticity, enhancing particle and energy transport [21–23]. Figure 1 shows two typical magnetic relaxation cycles during a single discharge in MST. Figure 1(a) shows U_{mag} during a 10 ms window. The magnetic fluctuation amplitudes for an unstable core-resonant $m = 1$, $n = 6$ mode (blue, dashed) and a nonlinearly driven edge-resonant $m = 0$, $n = 1$ mode (red, solid) are shown in Fig. 1(b), where m and n are the poloidal and toroidal mode numbers. The insets in Fig. 1 show the evolution (relative to MR) of U_{mag} (top) and magnetic fluctuation amplitudes (bottom) averaged over 485 MR events. At the MR event, 20–30 kJ of U_{mag} is released in 100 μs , and both core and edge-resonant mode amplitudes peak.

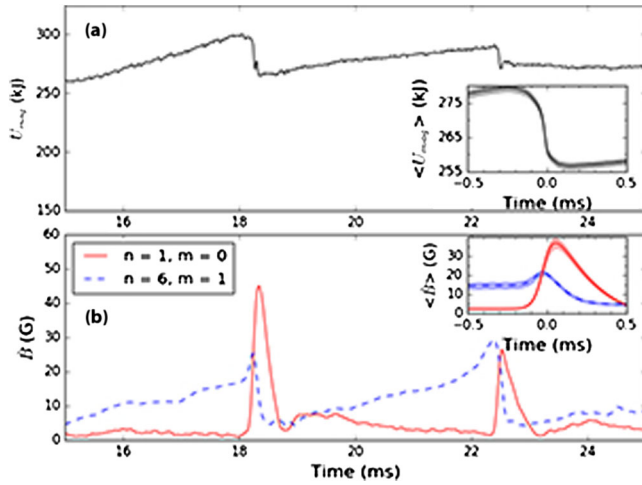


FIG. 1. (a) Evolution of U_{mag} for two magnetic relaxation cycles in a 500 kA standard plasma in MST. (b) Evolution of tearing mode amplitudes for the edge-resonant $m = 0$, $n = 1$ (red, solid) mode and the (innermost) core-resonant $m = 1$, $n = 6$ (blue, dashed) mode. The insets show the magnetic energy (top) and tearing mode amplitudes (bottom) averaged over 485 events (shaded region represents the standard error of the mean), with time relative to MR.

While ions are strongly energized during MR events (bulk heating and energetic ion tail formation) [17,18], the thermal population of electrons is measured by Thomson scattering to cool following MR [23,24]. Magnetic stochasticity is maximum during MR, and high mobility makes electrons susceptible to rapid transport. Hence, possible energization of electrons is anticipated to be transient on a $\sim 10 \mu\text{s}$ time scale, making high time resolution measurements necessary to reveal electron dynamics. We report energy-resolved bremsstrahlung emission showing an enhancement in the high energy x-ray flux during MR events in MST plasmas. Measurements were taken with a fast x-ray (FXR) diagnostic [25] that consists of a Si avalanche photodiode with optimal energy range of 3–25 keV and a 20 ns Gaussian shaping time.

We first describe x-ray bremsstrahlung emission measured through a $150 \mu\text{m}$ thick beryllium (Be) window with a line of sight along a minor radial chord with angular acceptance $\sim 15^\circ$ (Fig. 2, blue), intersecting the magnetic axis (called the radial view hereafter). Data were collected for plasmas with electron density $n_e = 0.8 \times 10^{19} \text{ m}^{-3}$ and plasma current $I_p = 500 \text{ kA}$ ($B \sim 3 \text{ kG}$). The electron temperature in the core is $T_e(0) \sim 500 \text{ eV}$. Figure 3 shows the energy-resolved x-ray flux versus time relative to the MR event ($t = 0 \text{ ms}$) for an ensemble of 485 MR events like those in Fig. 1, where black represents no measurable flux and red signifies high flux. The x-ray flux for $E > 20 \text{ keV}$ increases around $t = 0$, indicating that energetic electrons are generated during MR. After the MR event, the high energy x-ray flux decays rapidly, implying the energetic electrons are quickly lost, consistent with expectations for stochastic transport.

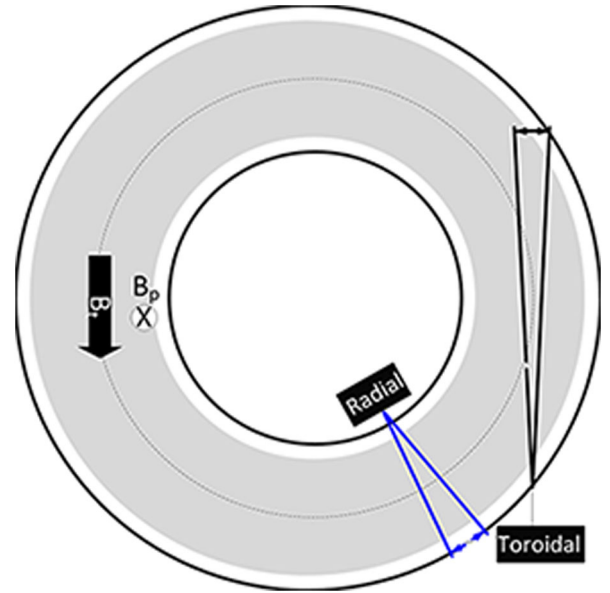


FIG. 2. A schematic of the FXR detector views.

To quantify the extent of energization, the x-ray distribution is averaged in $20 \mu\text{s}$ windows around the MR event between 5 and 25 keV. Figure 4 shows x-ray spectra for 0.5 ms before (black), during (red), and 0.5 ms after (blue) MR. The error bars in Fig. 4 (and Fig. 6 below) are calculated from the uncertainty in the number of x-ray counts, \sqrt{n} (standard deviation for Poisson distributions). To model the flux (Γ) as a function of energy, each spectrum is fit with a power law, $\Gamma(E) \propto E^{-\gamma}$, where γ is the tail spectral index. The smaller the γ , the greater the number of energetic x-rays are generated and the flatter the tail becomes. The error in γ (hereafter) is estimated from the variance-covariance matrix of the least squares power-law fit for each spectrum. For the spectra in Fig. 4, γ in the

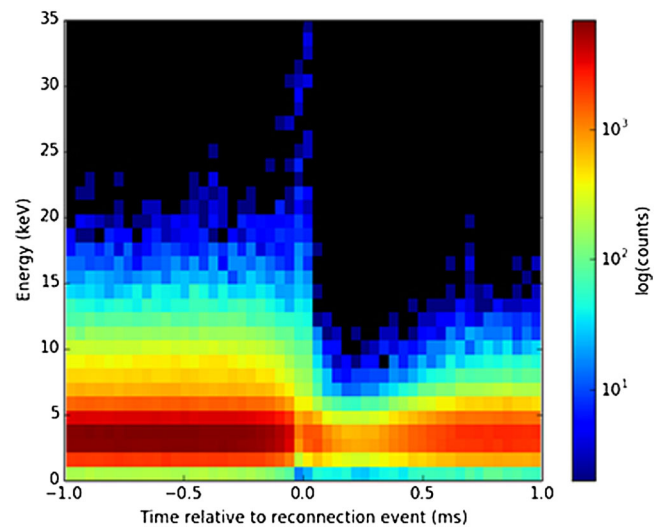


FIG. 3. The evolution of x-ray energy relative to MR (0 ms), with colors indicating x-ray flux. Black indicates no flux and dark red indicates high flux.

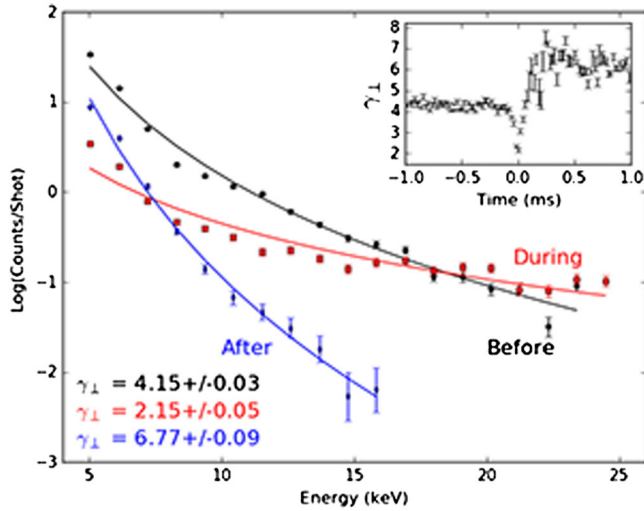


FIG. 4. X-ray spectra measured in the radial view for 20 μ s windows 0.5 ms before (black), during (red) and 0.5 ms after (blue) MR. Each spectrum is fit with a power law (solid lines), from which γ_{\perp} is calculated. The inset shows γ_{\perp} as a function of time relative to MR.

radial view (γ_{\perp}) decreases from 4.15 ± 0.03 to 2.15 ± 0.05 during MR, indicating significant flattening of the high energy tail. After the MR event, γ_{\perp} increases to 6.77 ± 0.09 , indicating the nonthermal electrons are lost from the plasma. The inset of Fig. 4 shows γ_{\perp} in 20 μ s intervals. Before the MR event, γ_{\perp} is constant, but decreases when the U_{mag} begins decreasing ($t \sim -70 \mu$ s). In as little as 60 μ s, γ_{\perp} reaches a minimum before there is a loss in high energy x-ray flux.

In principle, runaway acceleration of electrons due to the inductive electric field parallel to \mathbf{B} could produce an energetic x-ray tail in MST plasmas. Experiments in the PLT tokamak studying the angular distribution of bremsstrahlung emitted from runaway electrons showed that x-ray emission peaks in the direction in which electrons travel, leading to a measured toroidal anisotropy in the x-ray velocity distribution [11]. Modeling of the bremsstrahlung angular distribution shows this anisotropy occurs for electron energies as low as 10's of keV [26]. If the observed electron energization in MST plasmas is associated with runaway acceleration, the x-ray emission should peak in the direction of the parallel electric field, leading to an anisotropic bremsstrahlung angular distribution. To simulate the expected x-ray flux for electron runaway, we use the CQL3D code (a relativistic collisional quasilinear 3D Fokker-Planck solver [27]) to model a stationary test electron distribution with a mock runaway tail having a power-law energy distribution localized in v_{\parallel} with density $\sim 1\%$ of a background thermal (500 eV) Maxwellian distribution [Fig. 5(a)]. The mock tail has a Gaussian radial profile centered on the magnetic axis with a 9 cm radial extent. The code includes a calculation of x-ray bremsstrahlung along prescribed pencil-like lines of sight

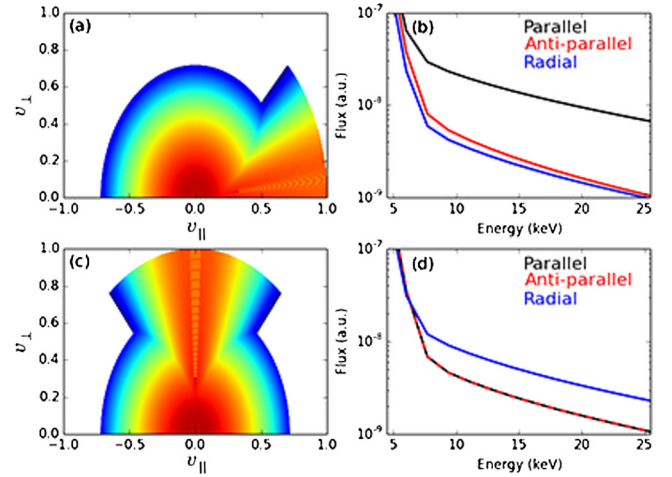


FIG. 5. (a) EDF used in CQL3D to model parallel anisotropy for a power-law tail distribution in v_{\parallel} . (b) Modeled bremsstrahlung x-ray emission for toroidal parallel (black), toroidal antiparallel (red), and radial (blue) pencil-like lines of sight. (c) EDF used in CQL3D to model perpendicular anisotropy for a power-law tail distribution localized in v_{\perp} . (d) Modeled bremsstrahlung x-ray emission for the same lines of sight as in (b). For both cases, the tail is Gaussian and v_{\parallel} and v_{\perp} are normalized to $v_{\text{norm}} = 1.9 \times 10^8$ m/s. The modeled emission is normalized for volume of viewing cones through the plasma core.

through the toroidal plasma volume, like that shown in Fig. 2. Figure 5(b) shows the modeled x-ray spectra for toroidal lines of sight on the midplane tangential to the magnetic axis that view on-coming (parallel, black) and receding (antiparallel, red) tail electrons. A radial (blue) line of sight through the magnetic axis is also shown. The x-ray flux in the toroidal views favors the parallel direction, as expected [11].

To look for asymmetry in the x-ray flux in MST plasmas, the FXR detector was moved to a toroidal view port with a 150 μ m thick Be window and an acceptance angle of $\sim 5^\circ$ (Fig. 2, black) located just below midplane and centered on the magnetic axis. Experiments were performed with E_{\parallel} in the normal (parallel) and reversed (antiparallel) directions to assess asymmetry in the x-ray flux and underlying electron distribution function (EDF). Figure 6 shows the x-ray spectra for a 20 μ s window during MR for views in the parallel (black), antiparallel (red), and radial (blue) directions. The x-ray spectra measured in the toroidal views show tail formation, but they are parallel-antiparallel symmetric within measurement uncertainty, with $\gamma_{\parallel} = 3.92 \pm 0.12$ and $\gamma_{\text{anti-}\parallel} = 3.73 \pm 0.14$. Hence, runaway acceleration is not consistent with the measured x-ray tail created by MR. Note that the toroidal views are not strictly parallel to \mathbf{B} along the line of sight, but “ \parallel ” is used for simplicity. For these plasmas, runaway generation is not expected to be strong since the net emf acting on electrons is below the critical (Dreicer [28]) field, $E_D = n_e e^3 \ln \Lambda / 4\pi \epsilon_0^2 m_e V_{\text{the}}^2$. The net large-scale (magnetic

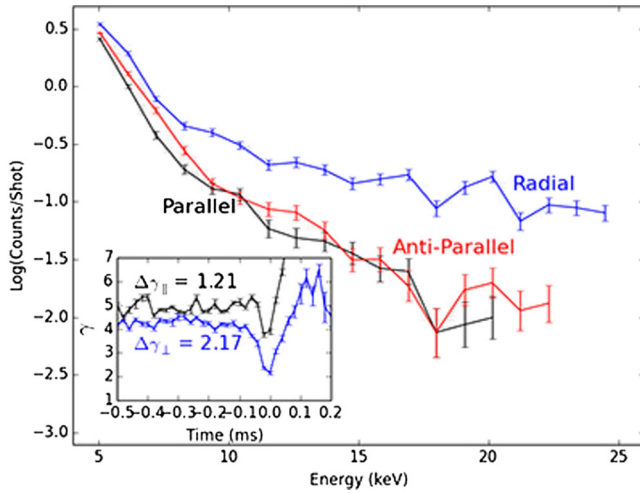


FIG. 6. X-ray spectra measured for parallel (black), antiparallel (red) and radial (blue) views during a $20 \mu\text{s}$ window during MR. The inset shows the evolution of γ for the parallel (black) and radial (blue) views.

flux-surface average) emf from all contributions in Ohm's law must be balanced by ηJ_{\parallel} , where η is the Spitzer resistivity and J_{\parallel} is the flux-surface-averaged parallel current density, both well known [23,29]. For these plasmas, $\eta J_{\parallel}/E_D \approx 0.12$. The electron tail contribution to J_{\parallel} is $<20\%$ [30].

In addition to toroidal symmetry, measurements show higher x-ray flux (and a more substantial high energy tail) in the radial view than in the toroidal views for $E > 10$ keV during MR. This is also contrary to an EDF that has parallel anisotropy as indicated by the modeling above, which predicts the x-ray flux in the radial view to be an order of magnitude less than the toroidal views [Fig. 5(b)]. The evolution of the experimentally observed γ_{\perp} (blue) and γ_{\parallel} (black) are shown in the inset of Fig. 6. To quantify tail generation, $\Delta\gamma = \gamma_{\text{before}} - \gamma_{\text{during}}$ is calculated before and during MR, with larger $\Delta\gamma$ indicating a larger tail. The $\Delta\gamma$ in the radial view ($\Delta\gamma_{\perp} = 2.17 \pm 0.02$) is almost twice as large as in the toroidal view ($\Delta\gamma_{\parallel} = 1.21 \pm 0.02$). Also, note that the tail generation occurs in a narrower time window for toroidal views than for the radial view, indicated by the width of γ around 0 ms. The full width half maximum of γ_{\perp} is $65.9 \pm 3.3 \mu\text{s}$ compared to $39.1 \pm 1.6 \mu\text{s}$ for γ_{\parallel} . Also, the decrease in γ_{\parallel} is delayed relative to γ_{\perp} , and γ_{\parallel} relaxes faster than γ_{\perp} following MR, suggesting an energization process that favors the perpendicular direction, with pitch angle scattering into the parallel direction, followed by relatively rapid parallel transport. Previous ion energization measurements in MST also show anisotropy favoring a perpendicular heating mechanism [18]. The strong correlation with tearing dynamics suggests a turbulent mechanism is similarly active for electron tail energization, although the precise mechanism could be different for electrons and ions.

To assess anisotropy favoring the perpendicular direction while maintaining toroidal symmetry, we model a stationary test EDF with an energetic tail having a power-law energy distribution localized in v_{\perp} , again with a density of 1% the background 500 eV Maxwellian distribution [Fig. 5(c)]. The Maxwellian EDF fills the whole plasma volume, but the radial profile of the tail is Gaussian, centered on the magnetic axis with a 9 cm radial extent. Figure 5(d) shows the predicted x-ray spectra for pencil-like lines of sight in the parallel (black), antiparallel (red), and radial (blue) views. The predicted spectra in the toroidal views are symmetric, and for $E > 10$ keV, the flux is larger in the radial view. Thus, an electron tail distribution with strong perpendicular anisotropy is consistent with measurements of bremsstrahlung emission during MR in MST plasmas. Broadening the radial extent of the core-localized tail in the test EDF causes the predicted x-ray flux in toroidal views to eventually become larger than in the radial view, while narrowing the radial extent increases the x-ray flux in the radial view further. This implies that the fast electrons in MST plasmas must be radially localized to ~ 9 cm of the magnetic axis. This might result in part from weaker stochastic transport in that region, e.g., the residual magnetic island structure associated with the innermost-resonant tearing mode might preserve the integrity of magnetic surfaces near the magnetic axis.

The electron tail correlates with the released U_{mag} during MR events. The stored U_{mag} within the plasma volume scales as $U_{\text{mag}} \sim I_p^2$, and the size of the MR event tends to be larger with lower n_e . X-ray measurements were obtained for a variety of plasmas with $I_p = 300\text{--}500$ kA and $n_e = 0.4\text{--}1.5 \times 10^{19} \text{ m}^{-3}$. The U_{mag} released during MR, ΔU_{mag} , is easily determined using reconstructions of the magnetic equilibrium [29]. During MR, $\Delta\gamma_{\perp}$ increases from $\Delta\gamma_{\perp} = 1.94$ for $\Delta U_{\text{mag}} \sim 15$ kJ to $\Delta\gamma_{\perp} = 2.73$ for $\Delta U_{\text{mag}} \sim 55$ kJ. The strength of ion energization exhibits a similar trend with ΔU_{mag} . The operation with $q(a) = 0$ mutes ΔU_{mag} and electron (and ion) energization, since resonant $m = 0$ modes that strongly couple to $m = 1$ modes are removed from the plasma.

In summary, high-time-resolution measurements of x-ray energy spectra provide the first evidence of the formation of an anisotropic energetic electron tail in a toroidal plasma during MR that is not attributable to runaway acceleration. The bremsstrahlung photon energies extend to 20–30 keV during tearing-driven MR in MST plasmas. The energetic tail is characterized by a power law with a spectral index, γ_{\perp} , which decreases from 4.15 to 2.15 during MR and rapidly increases following the event, consistent with stochastic transport expectations. The measured x-ray tail spectra are large in a radial view and parallel-antiparallel symmetric in toroidal views, which rules out runaway acceleration as the responsible mechanism. An anisotropic EDF with a population of fast

electrons localized in v_{\perp} and spatially limited to the core region is consistent with the measured x-ray energy spectra. The dynamics of the x-ray tail correlate with the dynamics of tearing modes and the magnitude of U_{mag} released by MR, implying a turbulent process is the most likely cause for the anisotropic energetic electron tail formation. These results provide laboratory plasma evidence for electron energization due to a process other than parallel electric fields during MR, similar to WIND spacecraft observations. Perpendicular energization is also observed for ions in MST, which suggests similar mechanisms may operate simultaneously on electrons and ions. These results also provide new opportunity to better understand the conversion of U_{mag} and particle dynamics, to improve theories that accurately describe MR and particle energization, and to strengthen the connections between MR processes observed in space and laboratory experiments.

The authors thank the UW-Madison MST group for the many valuable discussions. This material is based upon work supported by the U.S. Department of Energy Office of Science, Office of Fusion Energy Sciences program under Award No. DE-FC02-05ER54814 and the National Science Foundation under Grant No. PHY08-21899. MST data shown in this Letter can be obtained in Ref. [31].

*Corresponding author.

amidubois25@gmail.com

- [1] M. Hoshino, T. Mukai, T. Terasawa, and I. Shinohara, *J. Geophys. Res.* **106**, 25979 (2001).
- [2] M. Hoshino, K. Hiraide, and T. Mukai, *Earth Planets Space* **53**, 627 (2001).
- [3] M. Øieroset, R. P. Lin, T. D. Phan, D. E. Larson, and S. D. Bale, *Phys. Rev. Lett.* **89**, 195001 (2002).
- [4] J. Birn, A. V. Artemyev, D. N. Baker, M. Echim, M. Hoshino, and L. M. Zelenyi, *Space Sci. Rev.* **173**, 49 (2012).
- [5] Q. Pan, M. Ashour-Abdalla, R. J. Walker, and M. El-Alaoui, *J. Geophys. Res.* **119**, 1060 (2014).
- [6] R. P. Lin and H. S. Hudson, *Sol. Phys.* **17**, 412 (1971).
- [7] S. Masuda, T. Kosugi, H. Hara, S. Tsuneta, and Y. Ogawara, *Nature (London)* **371**, 495 (1994).
- [8] W. Fox, M. Porkolab, J. Egedal, N. Katz, and A. Le, *Phys. Plasmas* **17**, 072303 (2010).
- [9] I. Klimanov, A. Fasoli, and T. P. Goodman, *Plasma Phys. Controlled Fusion* **49**, L1 (2007).
- [10] P. V. Savrukhn, *Phys. Rev. Lett.* **86**, 3036 (2001).
- [11] S. Von Goeler, J. Stevens, S. Bernabei, M. Bitter, T. K. Chu, P. Efthimion, N. Fisch, W. Hooke, K. Hill, J. Hosea, F. Jobes, C. Karney, J. Mervine, E. Meservey, R. Motley, P. Roney, S. Sessnic, K. Silber, and G. Taylor, *Nucl. Fusion* **25**, 1515 (1985).
- [12] K. Yamasaki, S. Inoue, S. Kamio, T. G. Watanabe, T. Ushiki, X. Guo, T. Sugawara, K. Matsuyama, N. Kawakami, T. Yamada, M. Inomoto, and Y. Ono, *Phys. Plasmas* **22**, 101202 (2015).
- [13] M. Yamada, J. Yoo, J. Jara-Almonte, H. Ji, R. M. Kulsrud, and C. E. Myers, *Nat. Commun.* **5**, 4774 (2014).
- [14] X. Guo, M. Inomoto, T. Sugawara, K. Yamasaki, T. Ushiki, and Y. Ono, *Phys. Plasmas* **22**, 101201 (2015).
- [15] T. Ushiki, M. Inomoto, and H. Koguchi, *IEEE Trans. Fundam. Mater.* **134**, 493 (2015).
- [16] A. Retino, R. Nakamura, A. Vaivads, Y. Khotyaintsev, T. Hayakawa, K. Tanaka, S. Kasahara, M. Fujimoto, I. Shinohara, J. P. Eastwood, M. Andre, W. Baumjohann, P. W. Daly, E. A. Kronberg, and N. Cornilleau-Wehrin, *J. Geophys. Res.* **113**, A12215 (2008).
- [17] G. Fiksel, A. F. Almagri, B. E. Chapman, V. V. Mirnov, Y. Ren, J. S. Sarff, and P. W. Terry, *Phys. Rev. Lett.* **103**, 145002 (2009).
- [18] R. M. Magee, D. J. Den Hartog, S. T. A. Kumar, A. F. Almagri, B. E. Chapman, G. Fiksel, V. V. Mirnov, E. D. Mezonlin, and J. B. Titus, *Phys. Rev. Lett.* **107**, 065005 (2011).
- [19] R. N. Dexter, D. W. Kerst, T. W. Lovell, S. C. Prager, and J. C. Sprott, *Fusion Technol.* **19**, 131 (1991).
- [20] J. Sarff *et al.*, in *The Magnetized Plasma in Galaxy Evolution*, edited by K. T. Chyzy, K. Otmianowska-Mazur, M. Soida, and R.-J. Dettmar (Observatorium Astronomiczne, Uniwersytet Jagiellonski, 2005), pp. 48–55.
- [21] S. C. Prager, A. F. Almagri, S. Assadi, J. A. Beckstead, R. N. Dexter, D. J. Den Hartog, G. Chartas, S. A. Hokin, T. W. Lovell, T. D. Rempel, J. S. Sarff, W. Shen, C. W. Spragins, and J. C. Sprott, *Phys. Fluids B* **2**, 1367 (1990).
- [22] T. M. Biewer, C. B. Forest, J. K. Anderson, G. Fiksel, B. Hudson, S. C. Prager, J. S. Sarff, J. C. Wright, D. L. Brower, W. X. Ding, and S. D. Terry, *Phys. Rev. Lett.* **91**, 045004 (2003).
- [23] J. A. Reusch, J. K. Anderson, D. J. Den Hartog, F. Ebrahimi, D. D. Schnack, H. D. Stephens, and C. B. Forest, *Phys. Rev. Lett.* **107**, 155002 (2011).
- [24] R. M. Magee, Ph.D. thesis University of Wisconsin-Madison, 2011.
- [25] A. M. DuBois, J. D. Lee, and A. F. Almagri, *Rev. Sci. Instrum.* **86**, 073512 (2015).
- [26] J. Stevens, S. Von Goeler, S. Bernabei, M. Bitter, T. K. Chu, P. Efthimion, N. J. Fisch, W. Hooke, J. Hosea, F. Jobes, C. Karney, E. Meservey, R. Motley, and G. Taylor, *Nucl. Fusion* **25**, 1529 (1985).
- [27] R. W. Harvey and M. G. McCoy, The CQL3D Code, Proc. IAEA TCM on Advances in Sim. and Modeling of Thermonuclear Plasmas, pp. 489–526, Montreal (1992), available through USDOC/NTIS No. DE93002962.
- [28] H. Dreicer, *Phys. Rev.* **115**, 238 (1959).
- [29] J. K. Anderson *et al.*, *Phys. Plasmas* **12**, 056118 (2005).
- [30] R. O'Connell, D. J. Den Hartog, C. B. Forest, J. K. Anderson, T. M. Biewer, B. E. Chapman, D. Craig, G. Fiksel, S. C. Prager, J. S. Sarff, S. D. Terry, and R. W. Harvey, *Phys. Rev. Lett.* **91**, 045002 (2003).
- [31] See Supplemental Material at <http://link.aps.org/supplemental/10.1103/PhysRevLett.118.075001>, for the digital format of the data shown in this Letter.